A Compact and Simply-Constructed All-metal Circularly Polarized Ridge-Waveguide Slotted Antenna Array for Vehicle Mounted Satcom on the Move (SOTM) Communication Application

Xiaochuan Fang, Wei Wang, Yuyang Zheng, Zhi Zheng, Hongtao Zhang, and Guan-Long Huang, *Senior Member, IEEE*

***Abstract*—In this paper, a novel circularly polarized (CP) ridge-waveguide slotted antenna array is proposed for vehicle used Satcom on the Move (SOTM) applications. The antenna array is designed closely following the required factors for generating the circular polarization. The proposed antenna array is constructed on a symmetrical single-ridge slotted waveguide. Each antenna element consists of a pair of inclined slots opened on the narrow walls, and longitudinal slots opened on the bottom of the U-shaped wall of the waveguide. The inclined slots and the longitudinal slots are able to radiate orthogonal electric-fields independently with a phase-difference of 90°. After a vector superposition in the far-field by using this design, the circular polarization could be realized with extremely low axial ratio theoretically. Several essential parameters affecting the CP performance are also studied in this paper. To verify the feasibility of the proposed approach, a four-element CP antenna array is simulated, fabricated and measured. Results show that the obtained prototype achieves a measured impedance bandwidth of 14.74% from 9.24 GHz to 10.71 GHz with S11 < -10 dB, and a 3-dB axial ratio bandwidth of 19.1% from 9.0 GHz to 10.9 GHz.**

***Index Terms*—Circular polarization, ridge-waveguide, slotted antenna, satcom on the move (SOTM).**

I. Introduction

Vehicle mounted satcom on the move (SOTM) communication becomes an attractive research topic in vehicle technology. Among the SOTM system, antenna is an essential device that could significantly influence the capability of vehicular communication on-the-move between ground and space [1]-[3]. To ensure the quality of signal propagation between the satellite and the fast-moving vehicles, antennas are expected to have desirable performances, e.g., high efficiency, low side lobes and low cross polarization. On the other hand, a relatively low cost is also highlighted in a commercialized SOTM antenna, which would be a superiority compared with other antennas that have complex construction, e.g., two-dimensional phased array antenna [4]. Some typical vehicle mounted SOTM antenna, e.g., reflector antenna and lens antenna [5], [6], have huge volume and weight. Planar arrays based on the microstrip patch antennas have advantages in terms of low profile, light mass, small volume, etc. However, these antennas have relatively low radiation efficiency, or exhibits high sidelobe level [7], [8]. Another much-concerned challenge for vehicle mounted SOTM antenna is the ability to adapt to harsh environment, for instance, extreme weathers or mountainous and other complex terrains [9]. This in turn requires the antenna to have reliable structural robustness, strong heat dissipation and the ability of beam forming or beam steering. These requirements make reflector antennas, as well as microstrip-based antennas become more difficult to be adopted. In contrast, all-metal-based antennas, e.g., waveguide slotted antennas, are preferred candidates to handle these issues

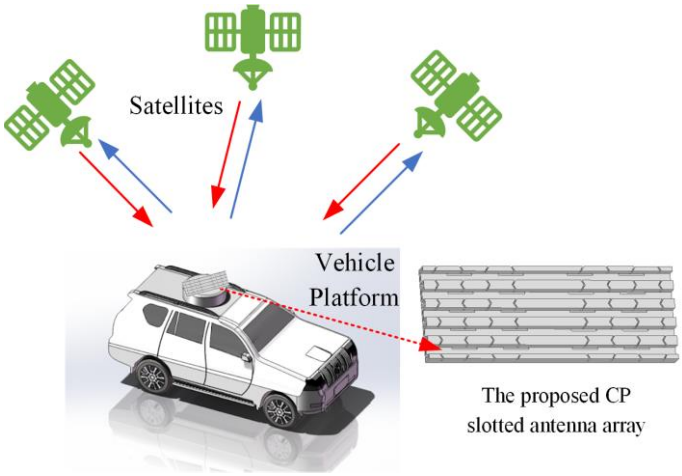

Fig. 1. Conceptual demonstration graph for the proposed antenna array deployed in SOTM application.

Manuscript submitted on. This work was supported by the National Natural Science Foundation of China (NSFC) under Grants 61801300 and 61671416. *(Corresponding author: Guan-Long Huang.)*

X.C. Fang is with the School of Electronic Engineering and Computer Science, Queen Mary University of London, London, UK (x.fang@qmul.ac.uk).

W. Wang is with the School of Microelectronics, Heifei University of Technology, Hefei 230009, Anhui, P.R. China. (e-mail: shu00ww@163.com).

Y.Y. Zheng, Z. Zheng and H.T. Zhang are with the East China Research Institute of Electronic Engineering, Hefei 230088, Anhui, P. R. China. (e-mail: shu00ww@163.com).

G.-L. Huang is with the School of AI-Guangdong & Taiwan, Foshan University, Foshan, Guangdong 528225, China (hgl@fosu.edu.cn).

[10], [11]. Nevertheless, waveguide-based antennas are not widely used in current commercialized vehicle mounted SOTM. This is because, similar to reflector antennas, waveguide-based antennas are bulky three-dimensional structures, resulting in a large volume and weight. Since the waveguide-based antenna is mainly used in the non-civilian scenarios, e.g., satellite, radar or military applications, the size and the weight reduction are seldom considered in most of the conventional waveguide-based antenna designs.

Circular polarized (CP) antennas are widely used in satellite communications. The polarization-rotatable electromagnetic (EM) wave produced by a CP antenna has several unique advantages, including excellent ability for anti-multipath fading, reduction of the Faraday rotation effect when signal propagates through the ionosphere, and better capability to let signal penetrate the atmosphere [12]. A circular polarized antenna can bring significant enhancement of communication quality in a vehicle mounted SOTM, especially considering the vehicle is moving at high speed, where the difficulty of polarization matching is dramatically increased. However, there is still few waveguide-based antenna that is reported to realize circular polarization, especially those with a relative compact volume. In fact, as there is no concern for wave-guided antenna volume and mass, loading external structures or layers on the existing waveguide antennas so as to transform linear polarization to circular polarization is a straightforward approach that is commonly used. Short monopoles [13], linear-to-circular polarization converters [14]-[16], open waveguides [17]-[19] and hybrid couplers [20], [21] are frequently used loading structures for generating the circular polarized waves. Evidently, these loading structures will further increase the volume and the weight of a waveguide-based antenna, which is hard to apply to a vehicle mounted SOTM. Loading external structures on a waveguide-based antenna will also deteriorate some critical performance which are expected by an advanced SOTM, e.g., beam steering ranges.

A waveguide-based antenna suitable for vehicle mounted SOTM is expected to have features of simple construction, low profile, compact volume and light mass, which means that an external loading structure is not acceptable for the antenna in generating the circular polarization. On the contrary, it is preferred that a single-layer waveguide-based antenna should be adopted. There are also some single-layer slotted leaky waveguide antenna arrays have been reported [22]-[28]. Among these designs, compound slots [22]-[26] or cross slots [27], [28] are opened on the waveguide to directly excite the CP waves. However, those antennas could only operate in traveling-wave mode. As a result, their working bandwidth are significantly limited, which makes them unsuitable to be used in the vehicle mounted SOTM, especially when high data transmission rate is required.

In this paper, a novel CP waveguide slotted antenna based on ridge-waveguide binate slot configuration is proposed for advanced vehicle mounted SOTM application. The proposed antenna is designed to operate at 10 GHz band. A conceptual demonstration graph of the proposed antenna array integrated into vehicle electronics is shown in Fig. 1. The proposed antenna achieves a remarkable progress on miniaturizing the cross-section size of 12 mm×9 mm with a low-profile. Unlike the previous designs using external structures/layers in waveguide-based antennas or applying multi-layer printed circuit board (PCB) structures, the proposed CP antenna have a significant simple structure for only composing of a single-layer U-shaped ridge-waveguide. Pairs of inclined slots are opened on the narrow walls of the ridge-waveguide, and longitudinal slots are placed on the bottom of the U-shaped waveguide wall. These two types of the slots are not only able to radiate the approximate intensity of EM fields independently, but also can generate orthogonal electric fields (*E*-field) with phase difference of 90°, which consequently fulfill the criteria of generating CP radiation. In addition to this work, the proposed antenna is designed and implemented closely following the conditions of forming circular polarization using waveguide's standing-wave mode. The proposed antenna also shows excellent advantages in low-profile, lightweight and easy fabrication, which make it become a promising candidate for future vehicle mounted SOTM applications.

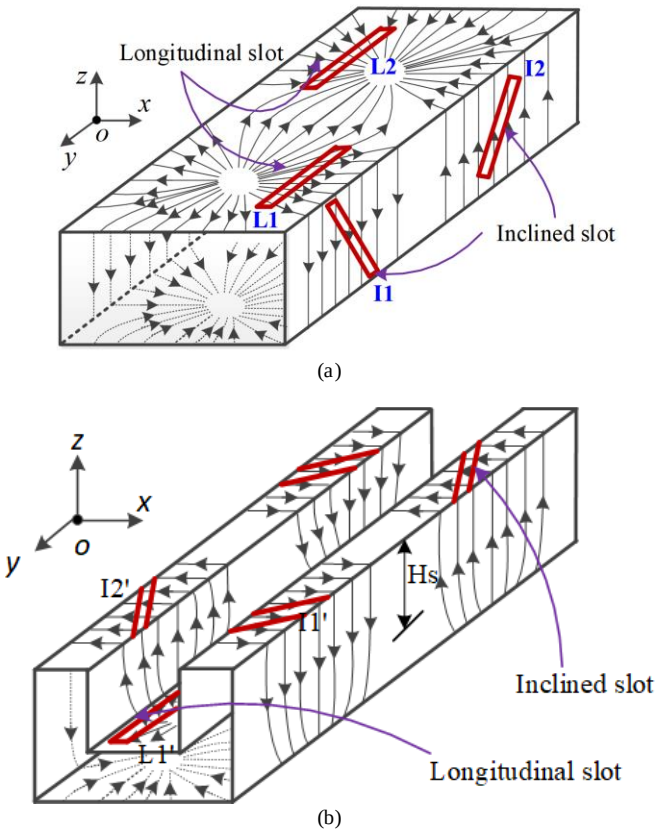

Fig. 2. Current distribution on different slotted waveguide. (a) Conventional rectangular waveguide. (b) Single-ridged waveguide.

II. Design Principle of CP Waveguide Slotted Antenna

This section presents the details of the design and working principle of the proposed CP antenna, which strictly follows the criteria of producing the circular polarization. For simplicity, it should be noted that all analyses presented in this work are based on a two-element waveguide slotted antenna model. According to the waveguide fundamental transmission characteristics, such an antenna could cover a complete

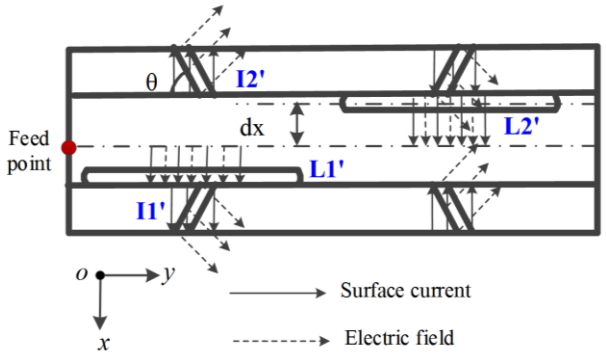

Fig. 3. *E*-filed and current distributions on different types of slots.

transmission phase period when the waveguide's dominant mode is TE_{10} mode.

According to the working mechanism, circular polarization could be formed by two orthogonal *E*-fields which have equal filed intensity and 90° phase difference. Therefore, a typical way to generate circularly polarized electromagnetic wave is synthesizing two orthogonal linear polarized electromagnetic waves, which have the same field intensity and 90° phase difference. Theoretically, the circular polarization is unable to be obtained from a conventional waveguide slotted antenna. As demonstrated in Fig. 2(a), a common rectangular waveguide slotted antenna obtains effective radiation either by opening the longitudinal slots on both sides of the broad waveguide wall, or by opening the inclined slots on the narrow waveguide wall, intentionally forcing the surface currents to be interrupted and radiated EM waves. However, these two kinds of surface currents interrupted by the corresponding slots are not able to provide proper *E*-fields to meet the requirements of forming circular polarization, which is mainly due to the following reasons. On one hand, if slots are purely opened on the same plane, e.g., Slots L1&L2 in *xoy*-plane or Slots I1&I2 in *yoz*-plane as shown in Fig. 2(a), they could only radiate linear polarized EM waves in the same broadside direction with equal field intensity. Nonetheless, as the composition of the *E*-field components of these linear polarized waves are along the same direction, such configuration is not possible to produce circular polarization. On the other hand, if the slots are opened on the broad and the narrow waveguide walls simultaneously, e.g., Slots (L1, L2, I1, I2), two orthogonal *E*-field components could be obtained after the composition of *E*-field vectors, i.e., Slots L1&L2 generate the *E*-field along *x*-axis while Slots I1&I2 generate the *E*-filed along *y*-axis. Accordingly, the EM waves radiated from the slots on the two walls are propagating in directions perpendicular to each other, i.e., *z*-direction for longitudinal slots and *x*-direction for the inclined slots. Therefore, such radiations are unable to be synthesized to form a proper far-field circular polarization in a broadside direction. Additionally, in a conventional waveguide slotted antenna which excites standing waves, *E*-fields radiated from the neighbored slots on the same plane are in the phase difference of 180°, e.g., L1&L2, while the *E*-fields radiated from the neighbored longitudinal slot and inclined slot, e.g., L1&I1, are in-phase. Both situations result in the impossibility of reaching a phase difference of 90° between the orthogonal *E*-fields,

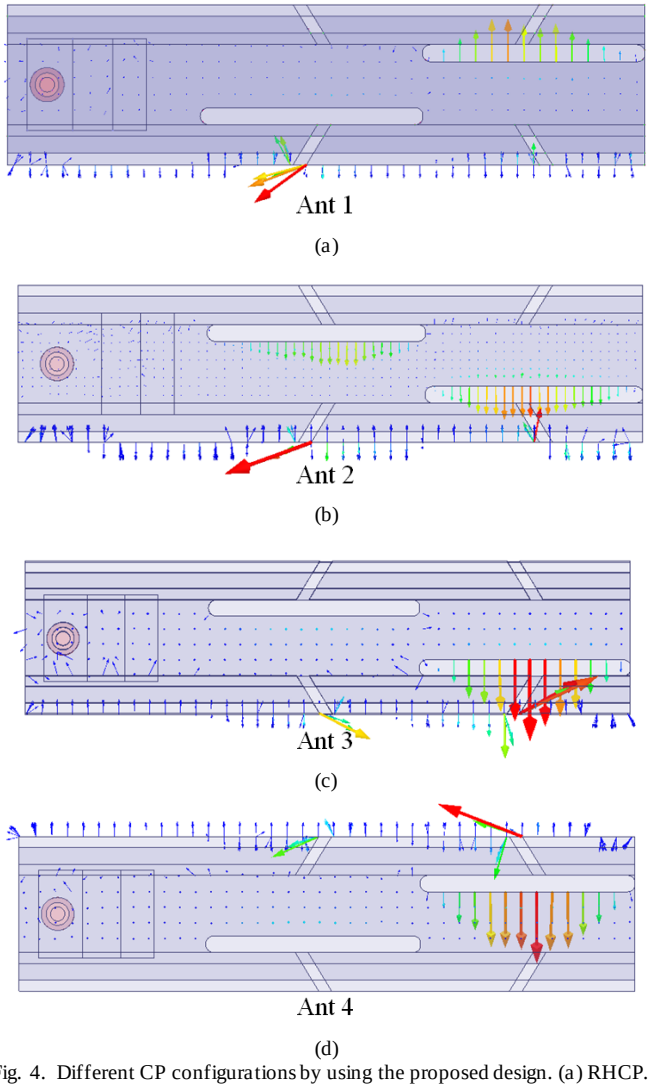

Fig. 4. Different CP configurations by using the proposed design. (a) RHCP. (b) LHCP. (c) RHCP. (d) LHCP.

making the function of circular polarization unattainable in the conventional waveguide slotted antenna.

To overcome the above technical dilemma, a modified waveguide slotted antenna realized by a single-ridged waveguide is presented in this work to implement the circular polarization. Fig. 2(b) exhibits the configuration of the novel single-ridged waveguide slotted CP antenna. The structural evolution of the proposed antenna is detailed as follows. For a conventional rectangular waveguide operating in the TE_{10} mode, one of the broad walls could be folded into a symmetrical U-shaped single-ridged waveguide but still maintaining its transmission characteristics. Based on the equivalence of the electrical length, subsequently, the longitudinal slots opened on the broad wall of the conventional waveguide could be transferred onto the bottom of the U-shaped ridge, e.g., observing the placement of the Slot L1 in Fig. 2(a) and the Slot L1' in Fig. 2(b). Similarly, the inclined slots opened on the narrow wall of the conventional waveguide could be transferred onto the top narrow wall of the of ridged waveguide, e.g., observing the location of the Slot I1&I2 in Fig. 2(a) and the Slot I1'&I2' in Fig. 2(b).

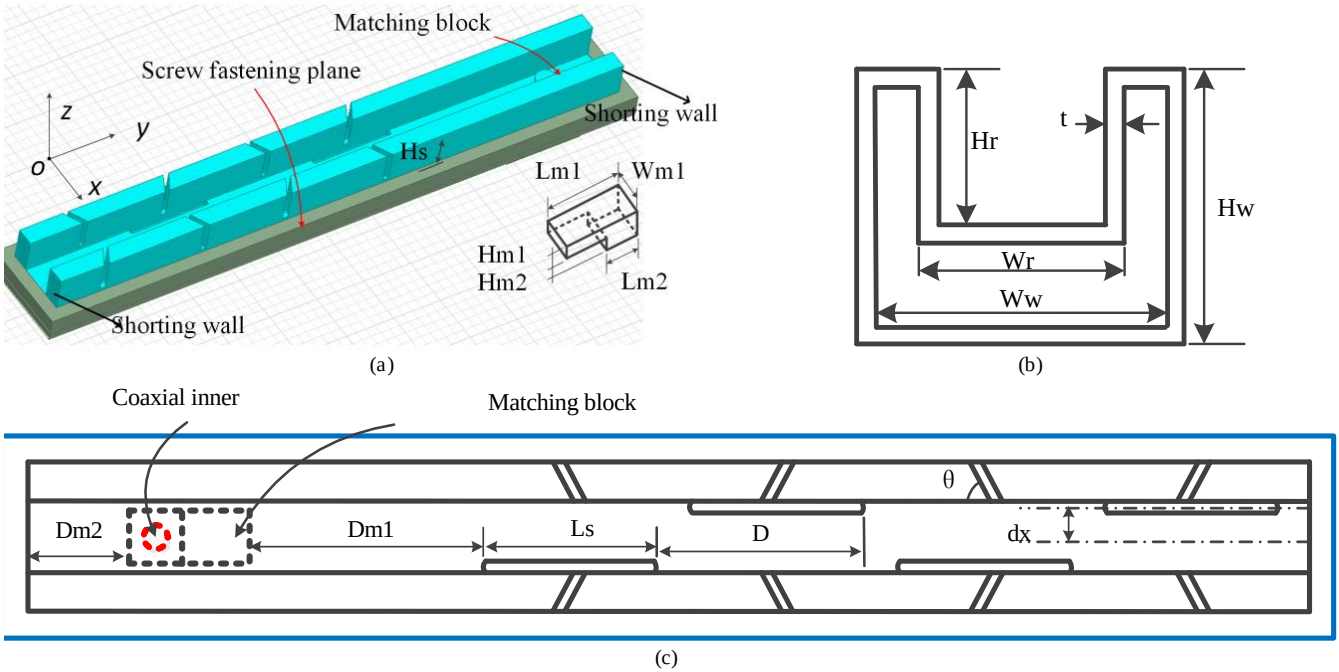

Fig. 5. Configuration of the proposed antenna array. (a) 3D view. (b) Cross-section view. (c) Top view.

By implementing the proposed structure, the requirements of producing the circular polarization can be easily fulfilled. Firstly, the currents across the longitudinal and the inclined slots are in the same direction, i.e., *x*-direction as shown in Fig. 2(b), which indicates the two types of excited *E*-fields coming from the slots' current interruption can be synthesized in broadside direction. Secondly, the phase difference of 90° between the two *E*-field components could be obtained from tuning the *z*-directional spacing between the longitudinal and the inclined slots. Thirdly, according to the working principle of slotted antennas, the direction of the *E*-field generated from the slot is generally parallel to its short edge. Hence, as shown in Fig. 3, the *E*-field components radiated from the longitudinal slots are parallel to the *x*-axis. The *E*-field components excited by the inclined slot could be divided into two vector components that parallel with the *x*-axis and the *y*-axis respectively. In particular, as considering the *E*-field components radiated from a pair of inclined slots (e.g., Slots I1'&I2' in Fig. 3) opened on both sides of the longitudinal slot (e.g., Slot L1' in Fig. 3), their vector decomposition components along *x*-axis would cancel each other out, while their components along *y*-axis are superimposed. As a consequence, the *E*-fields of a pair of inclined slots after vector composition can be treated as parallel to the *y*-axis. Namely, an orthogonal relationship between the *E*-field components can be established by combining the radiation characteristics of the longitudinal and the inclined slots. Lastly, the field intensity of the EM wave that radiated from the longitudinal slot could be adjusted by changing the displaced distance of the slot (denoted as dx in Fig. 3), while that radiated from the inclined slot could be tuned by rotating the slant angle (denoted as θ in Fig. 3) of the slot. It is worth mentioning that an outstanding advantage of the proposed design is that the field intensity generated from the two types of slots could be adjusted independently, allowing more freedom in the design process to achieve an approximately equal amplitude in the interested bandwidth.

In the proposed antenna, the resonance of the longitudinal slots and vertical slots are generated independently. The resonant frequency of the longitudinal slot is determined by their length, i.e. Ls. The resonant frequency of the inclined slot is determined by its effective electrical length, i.e. 2Hs+(Ww-Wr)/2/cosθ. The impedance resonant frequency of the longitudinal slots is designed to be lower than the AR resonant frequency of the proposed antenna, i.e. 10 GHz. The impedance resonant frequency of the inclined slots is designed to be higher than the AR that resonant frequency. The impedance bandwidth of this antenna is thus increased. On the other hand, the phase of the longitudinal slots is opposite with which of the inclined slots at 10.2 GHz. This brings a very low AR value at that frequency.

Therefore, based on the above analysis, circular polarization is realizable on the proposed ridged waveguide slotted antenna theoretically and numerically by properly exciting the orthogonal polarizations from the longitudinal and the inclined slots. And owing to the efficient designing approach, the proposed antenna could realize circular polarization with a much simpler and robust configuration, and none of external or multi-layer structures are required. Noted that axial ratio is normally used to evaluate the performance of circular polarization, which typically refers to the *E*-field amplitude ratio of the orthogonal polarized EM wave. In this work, as the EM waves are independently radiated from the longitudinal slots and the inclined slots, the AR of the proposed antenna is expected to be excellent theoretically. Additionally, the proposed design is easy to achieve different CP modes, i.e., left-hand circular polarization (LHCP) and right-hand circular polarization (RHCP), by simply altering the location and rotation of the longitudinal and inclined slots respectively. Fig.

4 shows some examples of adopting the proposed design to realize different CP modes. For instance, as the Ant1 shown in Fig. 4(a), it could be recognized the *E*-field phase of the adjacent longitudinal slot lags behind that of the inclined slot. As mentioned previously, the phase difference should be 90° around to form the required circular polarization. With EM waves radiated from the two types of slots properly, a RHCP can be generated in this case. Ant2 in Fig. 4(b), on the contrary, generates a LHCP. As the E-field phase of the inclined slot lags behind that of the adjacent longitudinal slot. With the similar principle, Ant3 generates a RHCP and Ant4 generates a LHCP. Therefore, only relatively simple procedures are required to complete the structural conversion between the above antennas.

III. Design of 1×4-Element Antenna Array

A. Antenna Array Configuration

In order to verify the performance of the CP ridged waveguide slotted antenna designed by the above-mentioned approach, a four-element linear antenna array working at RHCP mode is demonstrated in this section. The central frequency of this antenna array is fixed at 10 GHz for *X*-band SOTM application. Fig. 5 shows the structure of the proposed antenna array, where the parameters Ww and Hw are the width and the height of the waveguide wall, respectively. These dimensions can be determined by the equations elaborated in [29], as well as the technical principles detailed in [30]. In addition, Wr and Hr are the width and the height of the U-shaped ridge respectively, which are generally fixed by engineering experience values or equations, e.g., Wr = 0.45Ww. However, in the proposed antenna array, the height of the U-shaped ridge (Hr) would affect the performance of circular polarization. Therefore, parametric study on Hr, as well as other previously-mentioned parameters like the displaced offset of the longitudinal slot (dx) and the rotating angle of the inclined slot (θ), should be conducted to figure out proper values, some of which will be performed analysis in next sub-section. Meanwhile, the width of both types of slots, Ws, is set to 1 mm in this work, which is also adequate for fabrication requirements. In addition, the spacing between the neighbored longitudinal slots or the adjacent inclined slots along *y*-direction is denoted as D. This antenna array is designed to operate in the standing-wave mode, and the condition $D = 0.5\lambda_g$ should be strictly maintained, where λ_g is the waveguide wavelength at the center frequency, which could be calculated by:

$$\lambda_g = \frac{\lambda}{\sqrt{1-\left(\frac{\lambda}{\lambda_c}\right)^2}} \quad (1)$$

where λ is the free-space wavelength at 10 GHz, and λ_c is the cutoff wavelength of the ridged waveguide, which could be determined by the approach given in [29]. Lastly, for ease of machining fabrication, the thickness of the ridge waveguide (t) is set to 0.8 mm. The proposed antenna array is fed by a SMA connector. A metallic matching block under the ridge is utilized for impedance transform. Sizes of the matching block are denoted by Lm1, Lm2, Hm1, Hm2 and Wm1, as shown in Fig. 5(a). In addition to optimizing the matching block alone, its distance from the shorting wall (Dm2) also needs to be fine-tuned, which should be around a quarter-wavelength theoretically.

TABLE I
PARAMETERS OF THE PROPOSED ANTENNA ARRAY

Parameters	Ww	Hw	Wr	Hr	Ls	Ws
Values (mm)	12	9	8.66	6.9	16.6	1
Parameters	dx	θ	Hs	D	Lm1	Wm1
Values (mm)	3	31.4°	6.1	19.47	11.3	5.17
Parameters	Lm2	Hm1	Hm2	Dm1	Dm2	t
Values (mm)	4.71	0.5	0.5	22.09	8.04	0.8

As abovementioned, the overall design progress can be summarized as the following steps. (1) The main radiating structures, including the ridged waveguide and the two types of slots, are constructed and simulated. An ideal waveguide port can be applied to feed the antenna array at this stage. (2) The impedance matching structure for ridged waveguide feeding, i.e., the matching block as shown in Fig. 5, is designed independently. A waveguide-to-coaxial transition has to be considered during the simulation. (3) In order to take practical assembly into consideration, a screw fastening plane is applied to combine the antenna array and the matching block together. Such combined structure is required to be evaluated to realize the desired performance.

B. Para metric Analysis of the Antenna Array

As the height of the ridge, Hr, namel y the distance of the inclined slots above the longitudinal slots, plays an important role in the phase difference of the *E*-field components between the two types of slots, it is firstly studied in this sub-section. To obtain the phase difference of 90°, the surface current length between the neighbored inclined slot and longitudinal slot should be approaching $0.25\lambda_g$. Figs. 6(a) and (b) exhibits the parametric study of AR and reflection coefficient (represented by S11) of the antenna array with various Hr values. As can be seen, this parameter has great impact on both the AR and S11 performance, indicating Hr has close relationship with λ_g. Consequently, the optimized value o f Hr provided by HFSS is 6.9 mm, which is quite close to the calculated value of 6.77 mm.

As discussed earlier, the displaced offset of the longitudinal slot (dx) and the rotating angle of the inclined slot (θ) have influence on the *E*-field amplitude of the EM wave that radiated from the two types of slots respectively. The best circular polarization is obtained under one of the conditions that the *E*-field amplitudes from different slots are the same. Figs. 6(c) and (d) verify that the AR fluctuates a lot with different dx values, while they only have limited effect on the impedance matching as the value changing step is small. Noted that the analysis of the parameter θ is not shown in the paper as it returns to similar phenomenon as dx.

In addition, several parameters relevant to the antenna radiation performance are also analyzed, i.e., the length of the longitudinal slots (Ls) and the depth of the inclined slots (Hs). Theoretically, Ls should be less than λ to avoid the appearance of grating-lobes. Meanwhile, it has been proved that the resonance characteristics of a waveguide slotted antenna

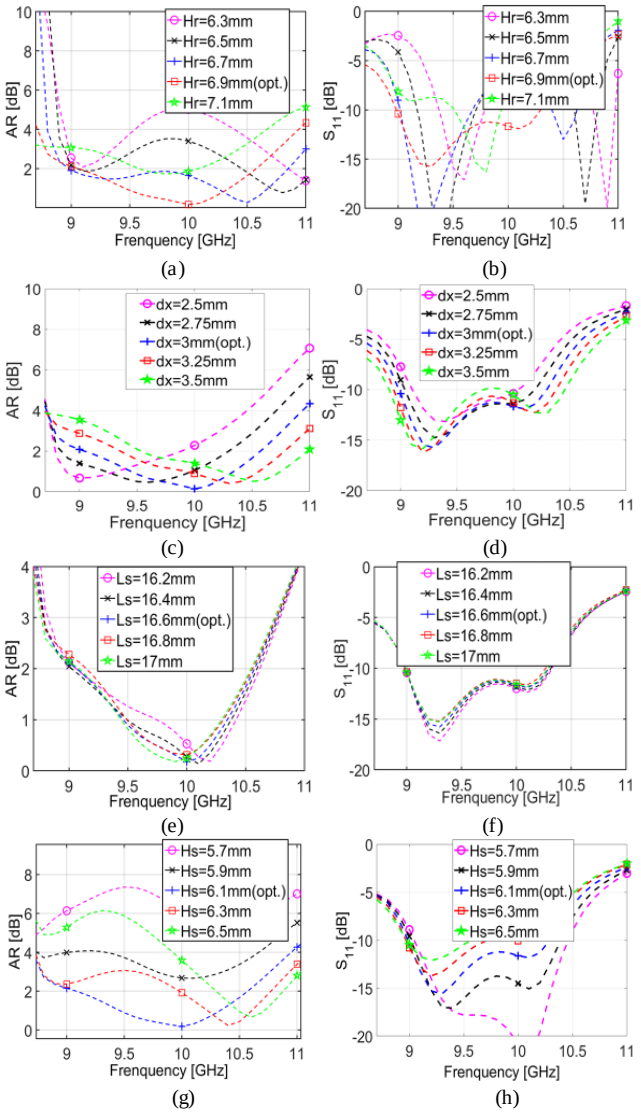

Fig. 6. Parametric study of the proposed antenna. (a) AR vs. Hr. (b) S11 vs. Hr. (c) AR vs. dx. (d) S11 vs. dx. (e) AR vs. Hs. (f) S11 vs. Hs.

operating in standing-wave mode would not be affected by the length of the longitudinal slot [31]. Accordingly, Figs. 6(e) and (f) prove such phenomenon in the proposed design. Either the AR or S11 of the antenna array only shows minor fluctuation as Ls varies. On the other aspect, changing the depth of the inclined slot (Hs) does not affect λ_g, which is different from the parameter Hr, but it still contributes to the frequency resonance and the AR performance, as shown in Figs. 6(g) and (h). As shown in Fig. 6(g), the AR values dramatically changes with different Hs values, the phenomenon of which is mainly due to amplitude mismatch between the *E*-fields produced by the two types of slots. Also, a significant resonance variation at the high frequency point (around 10.15 GHz) is observed in Fig. 6(h), while that at the low frequency point (around 9.25 GHz) is slightly affected. This analysis confirms that the high frequency resonance is generated by the inclined slots, while the resonance at low frequency is excited by the longitudinal slots, revealing the two resonances can be independently adjusted to achieve a wide bandwidth covering the band of interested. Table I tabulates the final parametric values of the proposed antenna array.

IV. Measurement Results

In order to verify the practical performance of the proposed CP antenna array, a 4-element antenna array has been prototyped and performed EM measurement. The prototype is made up of aluminum alloy by using milling process, as shown in Fig. 7. The antenna array is separated into two parts in fabrication, i.e., the radiating layer and the ground plate, which are ma nufactured respectively and assembled by screws.

The reflect on coefficient of the antenna array is measured by a vector network analyzer, and the radiation performance is evaluated in an anechoic chamber. A comparison between the results of the simulated and measured reflection coefficients is presented in Fig. 8, from which it can be seen that the measured impedance bandwidth of the proposed antenna array is 14.74% from 9.24 GHz to 10.71 GHz, showing a good agreement with the simulated result of 13.72% from 9.22 GHz to 10.6 GHz. Minor discrepancy between the two results is mainly caused by the manufacturing and the assembling tolerances. Figs. 9(a)-(f) show the CP radiation patterns of the proposed antenna array in the two main cut-planes, i.e., *xoz*- and *yoz*-planes, at 9.0 GHz, 10.0 GHz and 11.0 GHz respectively. It can be observed that the experimental results of the radiation patterns are in good

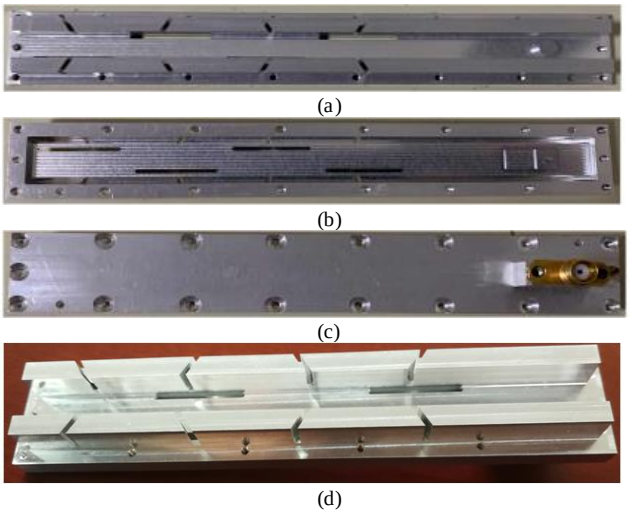

Fig. 7. Prototype of the 4-element CP antenna array. (a) Top view of the radiating layer. (b) Bottom view of the radiating layer. (c) Ground plate with SMA connector. (d) 3D view of the antenna array after assembly.

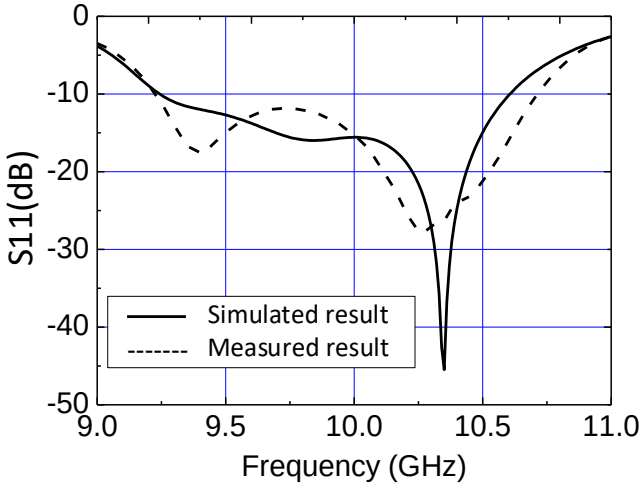

Fig. 8. Comparison between the simulated and measured reflection coefficient.

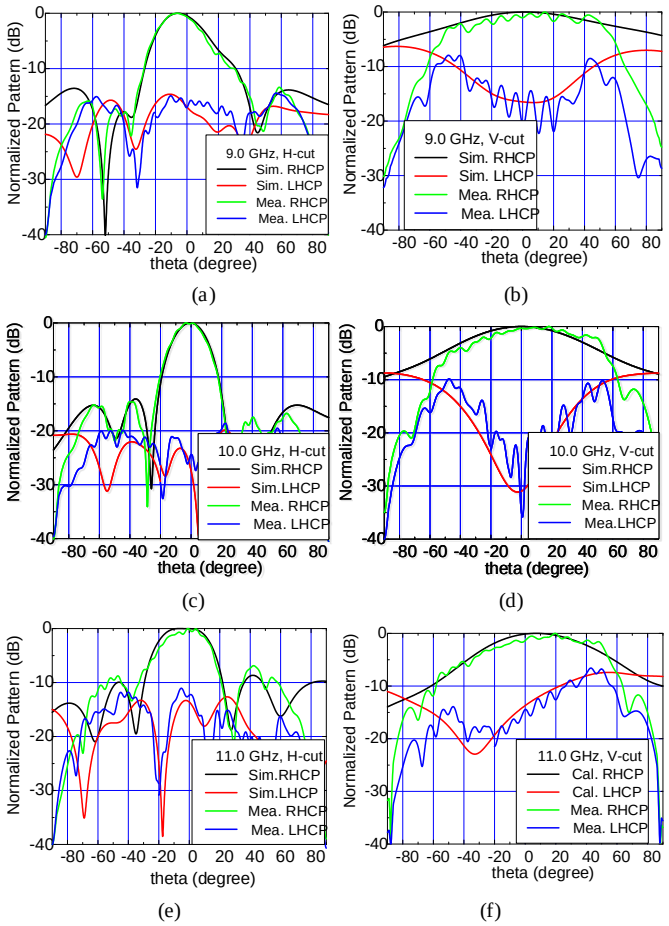

Fig. 9. Comparison between the simulated and measured radiation patterns of the array. (a) *xoz*-plane at 9 GHz. (b) *yoz*-plane at 9 GHz. (c) *xoz*-plane at 10 GHz. (d) *yoz*-plane at 10 GHz. (e) *xoz*-plane at 11 GHz. (f) *yoz*-plane at 11 GHz.

consistency with the simulated ones.

Fig. 10 shows the peak gain of this antenna array measured in the frequency band of 9-11 GHz, where the simulated results are also included for comparison. The experimental results show the array gain ranges from 10.16 dBc to 12.1 dBc in 9.3-10.5 GHz. In addition, a set of benchmarks of antenna efficiencies based on the calculated directivity is provided in Fig. 10, which allows us to identify the antenna efficiency from its gain curve. In this way, the measured efficiency of the antenna array varies between 69.02%-85.31% in the frequency range from 9.3 GHz to 10.5 GHz. Furthermore, Fig. 11 presents the simulated and measured AR of the antenna array. From the results, one can observe that the measured data are well approaching to the simulated ones, where the minimum AR value appears at around 10 GHz, verifying the feasibility of the abovementioned design approach. Particularly, a 3dB AR bandwidth of 19.1% covering from 9.0 GHz-10.9 GHz has been obtained from the measurement. Overall, all the experimental results in terms of operating bandwidth, radiation patterns and AR show that the proposed antenna array is able to provide good CP performance. Table II compares the proposed CP antenna array with some reported designs operating in standing-wave mode, from which it could be concluded that the proposed antenna array owns advantages of wider impedance and AR bandwidths with consideration of simpler structure.

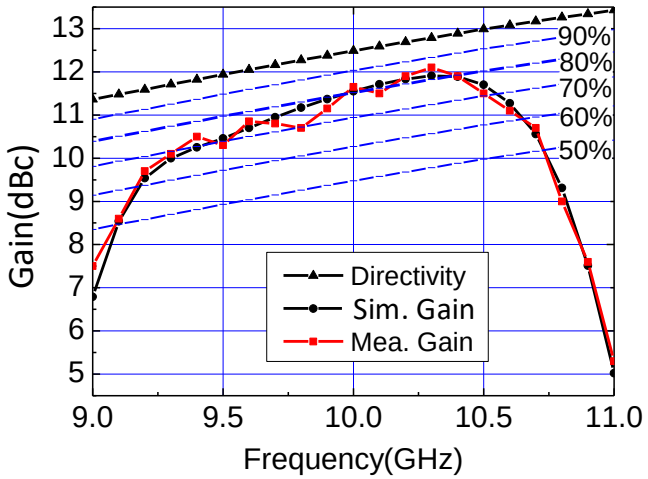

Fig. 10. Results of the simulated and measured gain (Size of radiation aperture: $12\times72.14\ mm^2$).

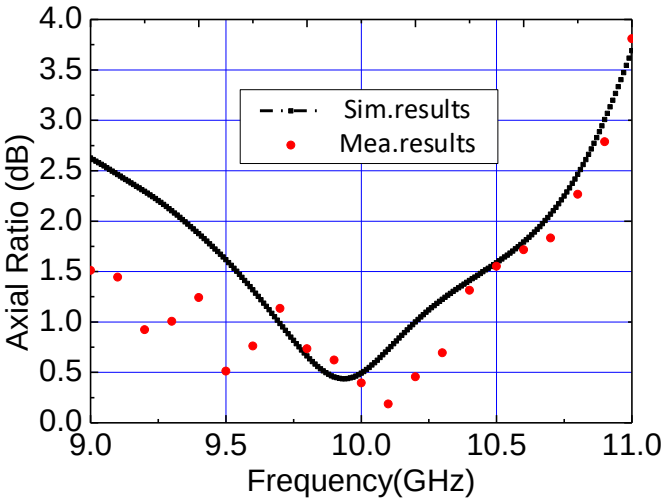

Fig. 11. Results of the simulated and measured AR.

TABLE II
PERFORMANCE COMPARISON BETWEEN THE PROPOSED AND REPORTED CP ANTENNA ARRAY

	Freq. (GHz)	Imp. BW (%)	AR BW (%)	Peak Gain (dBi)	Eff. (%)	Cross section dimensions (mm)	Aperture efficiency (%)
This work	10.0	14.74	19.1 (3 dB)	12.1	85.31 (Max.)	14×11	88.2 Max)
Ref. [10]	8.45	/	1.2(2dB)	26.1	62	325×300	84
Ref. [15]	20.45	7.3	7.3(1.1dB)	28.01	74.65 (Max)	10.81×18.41	36.06 Max)
Ref. [16]	10.5	4	3.2(3dB)	15.94	N/A	22×9	62

Freq.: frequency; Imp.: impedance; BW: bandwidth; Eff.: efficiency.

V. CONCLUSION

A novel compact and simply constructed all-metal circular polarized waveguide slotted antenna array operating in the standing-wave mode for vehicle mounted S OTM application is presented in this work. The detailed analysis of designing the circular polarization performance is also provided. A 4-element

waveguide slotted antenna array is numerically simulated and experimentally measured to verify the effectiveness of the proposed design approach. Results show that the proposed antenna array can achieve satisfactory impedance and AR bandwidth with good efficiency. The proposed circular polarized antenna could become an excellent candidate for future vehicle mounted SOTM applications.

REFERENCES

[1] Z. Wu, M. Yao, H. Ma, W. Jia, and F. Tian, "Low-Cost Antenna Attitude Estimation by Fusing Inertial Sensing and Two-Antenna GPS for Vehicle-Mounted Satcom-on-the-Move," *IEEE Trans. Veh. Technol.*, vol. 62, no. 3, pp. 1084-1096, Mar. 2013.

[2] A. Zaghloul and O. Kilic, "Antenna system solution for uninterrupted satellite-on-the-move (SOTM) communications," *IEEE AP-S International Symposium*, Jun. 2003, pp. 353-356.

[3] J. Herranz-Herruzo, A. Valero-Nogueira *et al*., "Low cost switchable RHCP/LHCP antenna for SOTM applications in Ka-band," *EuCAP 2015*, Apr. 2015.

[4] G. Gültepe, T. Kanar, S. Zihir and G. Rebeiz, "A 1024-Element Ku-Band SATCOM Dual-Polarized Receiver With >10-dB/K G/T and Embedded Transmit Rejection Filter," *IEEE Trans. Microw. Theory Tech.*, vol. 69, no. 7, pp. 3484-3495, July 2021.

[5] B. Lesur, A. Maati and et al., "A Large Antenna Array for Ka-Band Satcom-on-the-Move Applications—Accurate Modeling and Experimental Characterization," IEEE Trans. Antennas Propag., vol. 66, no. 9, pp. 4586-4595, June. 2018.

[6] A. Weily and N. Nikolic, "Dual-Polarized Planar Feed for Low-Profile Hemispherical Luneburg Lens Antennas," *IEEE Trans. Antennas Propag.*, vol. 60, no. 1, pp. 402-407, Jan. 2012.

[7] S. Liberto, G. Goussetis and A. Christie, "Design of a Dual-Circularly-Polarized Stacked Patch Antenna for SOTM application at Ka-band," *EuCAP 2020*, Mar. 2020.

[8] Z. Liu, L, Ji, P. Geng and Q. Huang, "A dual-circularly-polarized antenna array for satcom-on-the-move system", *IEEE APCAP 2017*, Oct. 2017.

[9] L. Marcellini, R. Forti and G. Bellaveglia, "Future developments trend for Ku and Ka antenna for satcom on the move", *EuCAP 2011*, Apr. 2011.

[10] N. Chahat, B. Cook, H. Lim, and P. Estabroo, "All-Metal Dual-Frequency RHCP High-Gain Antenna for a Potential Europa Lander," *IEEE Trans. Antennas Propag.*, vol. 66, no. 12, pp. 6791-6798, Dec. 2018.

[11] X. Fang, W. Wang, G. Huang and et al, "A Wideband Low-Profile All-Metal Cavity Slot Antenna with Filtering Performance for Space-Borne SAR Applications," *IEEE Antennas Wireless Propag. Lett.*, vol. 18, no. 6, pp. 1278-1282, Jun. 2019.

[12] H.-T Zhang, W. Wang, Z. Zheng, M.-P. Jin, and X. -L. Liang, "A Novel Dual Circularly-Polarized Waveguide Antenna Array", *IEEE International Symposium on Antennas and Propagation & USNC/URSI National Radio Science Meeting*, Jul. 2018, pp. 509-510.

[13] D. L. Schuler and J. S. Lee, "Terrain Slope and Surface Roughness Studies using Circularly Polarized SAR Backscatter," IEEE International Geoscience and Remote Sensing Symposium Proceedings (IGARSS'98), Jul. 1998, pp. 2187-2189.

[14] K. S. Min, J. Hirokawa, K. Sakurai, M. Ando, N. Goto, "Single-layer dipole array for linear-to-circular polarization conversion of slotted waveguide array," *IEE Porc. Microw. Antennas propag.*, vol. 143, no. 3, Jun. 1996, pp. 221-216.

[15] M. F. Feerando-Rocher, J. I. Herranz-Herruzo, A. Valero-Nogueira, and V. M. Rodrigo, "Circularly Polarized Slotted Waveguide Array with Improved Axial Ratio Performance," *IEEE Trans. Antennas Propag.*, vol. 64, no. 9, pp. 4144-4148, Sept. 2016.

[16] J. Xu, M. Wang, H. Huang, and W. Wu, "Circularly Patch Array Fed by Slotted Waveguide," *IEEE Antennas Wireless Propag. Lett.*, vol. 14, pp. 8-11, 2015.

[17] H.-T. Zhang, W. Wang, M.-P. Jin, and Y.-Q. Zou. "Broadband Circularly- Polarized slotted Waveguide Array Antenna with Low Axial Ratio," *12th European Conference on Antennas and Propagation (EUCAP 2018)*, 9-13rd Apr. 2018, London UK, pp. 1-4.

[18] R. V. Gatti and R. Rossi, "A Dual-Polarization Slotted Waveguide Array Antenna with Polarization-Tracking Capability and Reduced Sidelobe Level," *IEEE Trans. Antennas Propag.*, vol. 64, no. 4, pp. 1567-1572, Apr. 2016.

[19] M. Sharkawy and A. Kishk, "Wideband Beam-Scanning Circularly Polarized Inclined Slots Using Ridge Gap Waveguide," *IEEE Antennas Wireless Propag. Lett.*, vol. 13, pp. 1187-1190, Jun. 2014.

[20] Y.-Q. Zou, H.-T. Zhang, W. Wang, and M.-P. Jin. "Dual Circularly Polarized Waveguide Antenna Array for Satellite Communications in the X Band," *International Symposium on Antennas and Propagation (ISAP2015)*, Hobart, Tasmania, Australia, Nov. 2015, pp. 399-401.

[21] S.-G. Zhou, G.-L. Huang, and T.-H. Chio, "A Lightweight, Wideband, Dual-Circular-Polarized Waveguide Cavity Array Designed with Direct Metal Laser Sintering Considerations," *IEEE Trans. Antennas Propag.*, vol. 66, no. 2, pp. 675-682, Feb. 2018.

[22] G. Montisci, M. Musa, and G. Mazzarella, "Waveguide Slot Antennas for Circularly Polarized Radiated Field", *IEEE Trans. Antennas Propag.*, vol. 52, no. 2, pp. 619-623, Feb. 2004.

[23] L. M. Paulsen and C. Rapids, "Waveguide Crescent Slot Array for Loss-Loss, Low-Profile Dual-Polarization Antenna," *US Patent*, US7436371B1, 2008.

[24] V. Ravindra, P. R. Akbar, M. Zhang, J. Hirokawa, H. Saito, and A. Oyama, "A dual-polarization X-band traveling-wave antenna panel for small-satellite synthetic aperture radar," *IEEE Trans. Antennas Propag.*, vol. 65, no. 5, pp. 2144-2156, May 2017.

[25] X. Wu, F. Yang, and J. Zhou, "Circularly Polarized Waveguide Antenna with Dual Pairs of Radiation Slots at Ka-Band," *IEEE Antennas Wireless Propag. Lett.*, vol. 16, pp. 2947-2950, Jun. 2017.

[26] M. A. Sharkawy and A. A. Kishk, "Wideband Beam-Scanning Circularly Polarized Inclined Slots Using Ridge Gap Waveguide," *IEEE Antennas Wireless Propag. Lett.*, vol. 13, pp. 1187-1190, 2014.

[27] J. Hirokawa, M. Ando, N. Goto, and et al, "A single layer slotted leaky waveguide array antenna for mobile reception of direct broadcast from satellite," *IEEE Trans. Veh.Technol.*, vol. 44, pp. 749–755, Nov. 1995.

[28] T. Hirano, J. Hirokawa and M. Ando, "Waveguide Matching Crossed-Slot," *IEE Proc.-Microw. Antennas Propag.*, vol. 150, no. 3, pp.143-146, Jun. 2003.

[29] T. Chen, "Calculation of the Parameters of Ridge waveguide," *IRE Trans. Microw. Theory Tech.*, vol. 5, no. 1, pp. 12-17, Jan 1957.

[30] J. Lu, H. Zhang, W. Wang, and et al, "Broadband Dual-Polarized Waveguide slot Filtenna Array with Low Cross Polarization and High Efficiency," *IEEE Trans. Antennas Propag.*, vol. 67, no. 1, pp. 151-159, Jan. 2019.

[31] W. Wang, S. Zhong, Y. Zhang and X. Liang, "A broadband slotted bridge waveguide antenna array," *IEEE Trans. Antennas Propag.*, vol. 54, no. 8, pp. 2416-2420, Aug. 2006.

Xiaochuan Fang received the B.E. degree and M. Eng degree in School of Information and Communication Engineering at University of Electronic Science and Technology of China (UESTC), Chengdu, China. He is pursuing his Ph.D. degree in School of Electronic Engineering and Computer Science at Queen Mary University of London, London, U.K. His research interests include reconfigurable microwave devices, liquid metal-based electronics and design and implementation of high-performance antennas.

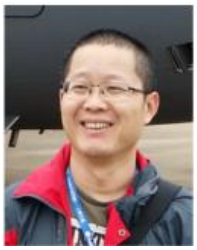

Wei Wang received the B.S. degree in Physics from Anhui University, Hefei, China, in 1993, the M.S. degree in electrical engineering from Xidian University, Xi'an, China in 2001 and the Ph.D. degree in electrical engineering from Shanghai University, Shanghai, China, in 2005. He is a Senior Member of the Chinese Institute of Electronics (CIE).

From 1993 to 1998 and from 2001 to 2002, he worked in the East China Research Institute of Electronic Engineering (ECRIEE), as an assistant engineer and an engineer,

respectively, where he is now a research professor. He also acts as the industrial cooperate professor in Heifei University of Technology, Anhui University and Shanghai Jiao Tong University, respectively. He has authored and co-authored one book, three book chapters, more than 50 journal papers, 60 conference papers and 47 Chinese patents. He received many awards, including one Second Class Awards for National Scientific and Technology Progress, two Second Class Awards for Scientific and Technology Progress of National Defense Industry, one First Class and one Third Class Awards for scientific and technology achievements in China Electronic Technology Group Corporation, one First Class award for Electronic Information Science and Technology of China Electronic Institute, one First Class and one Second Class Awards for Excellent Academic Papers in Natural Science of Anhui Province. His research interests include waveguide slot antennas, microstrip antennas for radar, compact ultra-wide-band (UWB) for wireless communications, microwave passive devices and circuits, and microwave/millimeter systems.

Yuyang Zheng received M. Eng degree in School of Electrical Engineering at University of Electronic Science and Technology of China (UESTC), Chengdu, China. He is an engineer in the East China research institute of electronic enginery. His research interests include circularly polarized antennas, broad band antennas and active arrays.

Zhi Zheng was born in Liaoning, China, in 1985. He received the B.S. degree in electronic information engineering, the M.S. degree in radio physics and the Ph.D. degree in radio physics in 2008, 2011 and 2015, respectively, all from Sichuan University. He currently works in the East China Research Institute of Electronic Engineering (ECRIEE), Hefei, China. His current research interests include waveguide slot antennas and microstrip antennas for phased array.

HongTao Zhang was born in Henan, China, in 1980. He received the B.S. degree in 2005, the M.S. degree in 2008, both in electronic engineering from Xidian University, Xi'an, China. Since 2008, he has been with the East China Research Institute of Electronic Engineering (ECRIEE), Hefei, China. He is currently an Antenna Research and Development senior engineer with the ECRIEE. His current research interests include phased array antennas, waveguide slot antennas, and ultra-wideband antennas.

Guan-Long Huang (M'11-SM'18) received the B.E. degree in electronic information engineering at Harbin Institute of Technology, Harbin, China, and the Ph.D. degree in electrical and computer engineering at National University of Singapore, Singapore. He is now a Full Professor with Foshan University, Foshan, Guangdong, China. He is also a joint-researcher with the Peng Cheng Laboratory, Shenzhen, Guangdong, China. Prior to join the current university, he has been with Shenzhen University as an Associate Professor, the Nokia Solutions and Networks System Technology as a Senior Antenna Specialist, and the Temasek Laboratories at National University of Singapore as a Research Scientist from 2011 to 2020. He was the TPC member and special session organizer of several international conferences. He has authored or co-authored more than 150 papers in journals and conferences. He was the recipient of the Raj Mittra Travel Grant (2021), the Best Reviewer Award of IEEE AWPL (2019) and IEEE TAP (2020, 2021), all from IEEE Antenna and Propagation Society, and the recipient of the Young Scientist Award in 2021 from Applied Computational Electromagnetics Society, the Fok Ying-Tong Education Foundation Award in 2020 from the Ministry of Education of the People's Republic of China, and the Foundation for Distinguished Young Talents in Higher Education of Guangdong Province, China in 2017. His research interests include design and implementation of high-performance antenna arrays, base-station and mobile RF front-end devices/antennas, millimeter-wave antenna, antenna measurement technique and 3-D printing technology in microwave applications.